

Analysis of the Meridional Energy Transport by Atmospheric Overturning Circulations

KRISTOFER DÖÖS AND JOHAN NILSSON

Department of Meteorology, Stockholm University, Stockholm, Sweden

(Manuscript received 5 March 2010, in final form 21 June 2010)

ABSTRACT

The atmospheric meridional overturning circulation is computed using the interim European Centre for Medium-Range Weather Forecasts Re-Analysis (ERA-Interim) data. Meridional mass transport streamfunctions are calculated not only using pressure as a vertical coordinate but also using temperature, specific humidity, and geopotential height as generalized vertical coordinates. Moreover, mass transport streamfunctions are calculated using the latent, the dry static, or the moist static energy as generalized vertical coordinates. The total meridional energy transport can be obtained by integrating these streamfunctions “vertically” over their entire energy range. The time-averaged mass transport streamfunctions are also decomposed into mean-flow and eddy-induced components. The meridional mass transport streamfunctions with temperature and specific humidity as independent variables yield a two-cell structure with a tropical Hadley-like cell and a pronounced extratropical Ferrel-like cell, which carries warm and moist air poleward. These Ferrel-like cells are much stronger than the Eulerian zonal-mean Ferrel cell, a feature that can be understood by considering the residual circulation related to specific humidity or temperature. Regardless of the generalized vertical coordinate, the present meridional mass transport streamfunctions yield essentially a two-layer structure with one poleward and one equatorward branch. The strongest meridional overturning in the midlatitudes is obtained when the specific humidity or the moist static energy is used as the vertical coordinate, indicating that the specific humidity is the variable that best distinguishes between poleward- and equatorward-moving air in the lower troposphere.

1. Introduction

Meridional overturning mass transport streamfunctions can be useful for describing the zonally averaged meridional atmospheric circulation. These streamfunctions delineate aspects of the three-dimensional circulation in two dimensions, which is advantageous for the purpose of visualizing. A possible mistake in interpreting overturning mass transport streamfunctions is to assume that their “streamlines” correspond directly to Lagrangian particle trajectories of the underlying three-dimensional flow. However, streamlines and Lagrangian trajectories coincide only in time-independent two-dimensional flows (Lichtenberg and Lieberman 1983). In the most common atmospheric description, the meridional mass transport overturning streamfunction is calculated using pressure as the vertical coordinate. This captures the zonally averaged

Eulerian circulation and gives the classical picture, illustrated in Fig. 1, with three overturning cells in each hemisphere (see, e.g., Peixoto and Oort 1992; Grotjahn 1993):

- the strong Hadley cells in the tropics with air in the lower troposphere moving equatorward while gaining heat and moisture from the ocean. The air ascends to the upper troposphere in the equatorial region and then moves poleward as it gradually cools and sinks, completing the overturning cell. These cells are thermally direct, implying that air is warmer in the ascending branch than in the descending branch.
- the weaker Ferrel cells in the midlatitude, which are associated with poleward motion near the surface and an equatorward return flow in the upper troposphere. These cells are thermally indirect, driven mechanically by transient eddies.
- very weak polar cells that are thermally direct.

In most of the Hadley cell region, the zonal-mean meridional overturning in pressure coordinates gives a leading-order approximation of the Lagrangian mass

Corresponding author address: Kristofer Döös, Department of Meteorology, Stockholm University, SE-10691 Stockholm, Sweden.
E-mail: doos@misu.su.se

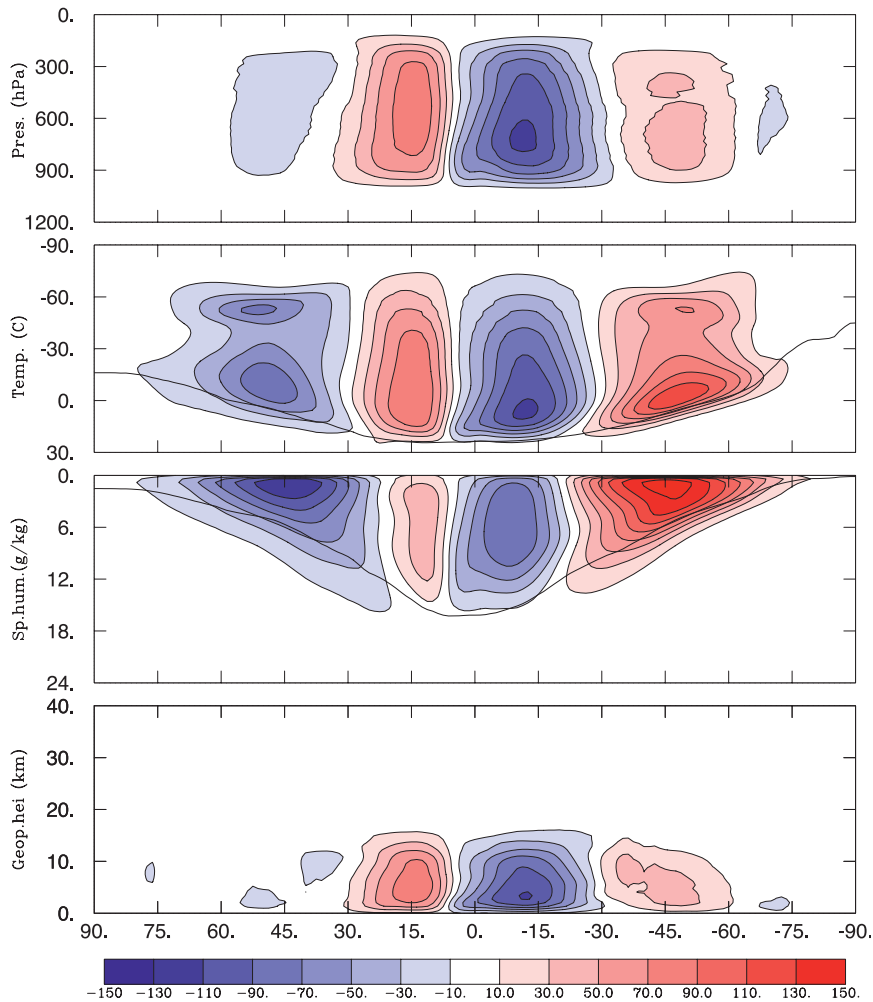


FIG. 1. The meridional overturning mass transport streamfunction as a function of pressure, temperature, specific humidity, and geopotential height. Streamline contours are every 20 Sv ($1 \text{ Sv} = 10^6 \text{ m}^3 \text{ s}^{-1}$ or 10^9 kg s^{-1}); positive values indicate anticlockwise circulation. These streamfunctions describe the total overturning averaged between 1989 and 2009 based on the ERA-Interim data. The superimposed black lines correspond to the zonally averaged time-mean temperature and humidity at the surface level. Note that, since the specific humidity generally decreases exponentially with altitude, the corresponding streamfunction primarily captures aspects of the circulation in the lower troposphere.

transport that carries energy and moisture meridionally (e.g., Held 2001; Diaz and Bradley 2004; Nilsson and Körnich 2008). In the thermally indirect Ferrel cells, on the other hand, this overturning streamfunction yields almost no information on the Lagrangian flow (see, e.g., Townsend and Johnson 1985; Grotjahn 1993). However, mass transport streamfunctions that better capture the Lagrangian circulation can be constructed by replacing the height coordinate with an appropriately selected scalar field (Bryan and Sarmiento 1985; Townsend and Johnson 1985; Hirst et al. 1996). One natural choice for the atmosphere is to replace the height coordinate with the potential temperature, that

is, one that measures the mass transport between the ground and a surface of constant potential temperature. The resulting streamfunction describes the mass transport in isentropic layers (Townsend and Johnson 1985). Another approach to obtain a more Lagrangian flow representation is to compute the transformed Eulerian mean, or residual, circulation (cf. Andrews and McIntyre 1976; Andrews et al. 1987). In fact, there are connections between residual circulations and overturning mass transport streamfunctions with generalized vertical coordinates: the standard residual circulation is an approximation in geometrical coordinates of the overturning circulation in isentropic coordinates (McDougall

and McIntosh 1996; McIntosh and McDougall 1996; Held and Schneider 1999).

The mass transport streamfunction based on potential temperature (or dry static energy) tends to yield a single thermally direct cell in each hemisphere that connects the high and the low latitudes (e.g., Townsend and Johnson 1985; Held and Schneider 1999; Czaja and Marshall 2006). This should be contrasted with the meridional overturning in pressure coordinates, which comprises several cells. The reason that the thermally indirect Ferrel vanishes in the isentropic representation is that in the midlatitudes it is the eddies, rather than the zonal-mean flow, that accomplish the meridional transport of mass and tracers (e.g., Townsend and Johnson 1985; Grotjahn 1993). In general, the zonal variations in meridional wind and potential temperature are correlated such that a net poleward (equatorward) mass transport occurs in isentropic layers with high (low) potential temperatures (see Fig. 3.18 in Grotjahn 1993). An oceanographic counterpart to the Ferrel cells is the Deacon cell in the Southern Ocean where the meridional overturning in vertical coordinates captures a thermally indirect circulation reaching from the surface down to several thousands of meters depth. However, when the overturning is projected on potential density–latitude coordinates, it almost entirely vanishes (Döös and Webb 1994; Karoly et al. 1997; Marshall and Radko 2006; Döös et al. 2008).

Recently, Pauluis et al. (2008, 2010) have studied the meridional overturning circulation using potential temperature and equivalent potential temperature as generalized height coordinates [see Czaja and Marshall (2006) for computations of the meridional overturning based on dry and moist static energy]. The analyses of Pauluis et al. show that the meridional overturning based on equivalent potential temperature better distinguishes between the poleward- and the equatorward-flowing branches in the midlatitudes, and, hence, yields a stronger mass transport than the overturning based on dry potential temperature. It should be noted that the equivalent potential temperature (as well as the moist static energy) generally has a minimum around the 600-hPa tropical troposphere and has a weak vertical gradient in the extratropics (see, e.g., Xu and Emanuel 1989; Czaja and Marshall 2006). Thus, the mass transport streamfunction based on equivalent potential temperature does not necessarily correspond to a simple overturning circulation in geometrical coordinates.¹ However, the

studies of Pauluis et al. (2008, 2010) also show that mass transport streamfunctions based on quantities that are not monotonic with height can highlight aspects of the general circulation: by selecting different generalized height coordinates one can obtain different vertical and zonal samplings of the meridional mass transport. Potentially this is useful for analyzing the general circulation if one bears in mind that the resulting overturning mass transport streamfunctions do not necessarily provide direct information on the overturning in geometrical coordinates.

In the present study, meridional overturning mass transport streamfunctions projected on various generalized height coordinates are used to analyze the general atmospheric circulation. One issue is to determine which features of the circulation can be captured using the meridional overturning in temperature T and specific humidity q coordinates. Another issue is to decompose the meridional overturning in energy coordinates into components due to dry static, latent, and moist static energies. Further, the generalized mass transport streamfunctions are decomposed into a mean-flow component and a time-varying eddy component. The present overturning analyses are based on data from the European Centre for Medium-Range Weather Forecasts (ECMWF): the interim ECMWF Re-Analysis (ERA-Interim) for the period 1989–2009 (Uppala et al. 2008). This reanalysis covers the data-rich period from 1989 onward and has an improved atmospheric model and assimilation system compared to the 40-yr ECMWF Re-Analysis (ERA-40). Simmons et al. (2007a,b), and Uppala et al. (2008) have demonstrated the important ERA-Interim improvements over ERA-40 in many areas, including the representation of the hydrological cycle and the strength of the Brewer–Dobson circulation, which have been identified as two special difficulties in ERA-40 (Uppala et al. 2005). The fit to observations and the quality of forecasts initialized with the ERA-Interim analyses have also been improved. The mass transport streamfunction computations reported in the present paper are made with 6-hourly outputs from the ERA-Interim dataset.

2. Meridional overturning mass transport streamfunction

The meridional overturning mass transport streamfunction can be defined in a general way for both the atmosphere and the ocean as a function of height or depth:

$$\Psi(y, z) \equiv \frac{1}{t_1 - t_0} \int_{t_0}^{t_1} \oint_{h(x,y)}^z \rho v(x, y, z', t) dz' dx dt, \quad (1)$$

¹ To some degree this also applies for mass transport streamfunctions based on potential temperature: Held and Schneider (1999) show that near-ground equatorward flow in midlatitudes occurs at potential temperatures lower than the surface zonal-mean value.

where ρ is the density and v the meridional velocity, t_0 and t_1 are the start and end of the time averaging period, and $h(x, y)$ is the surface of the earth or the bottom of the ocean. This streamfunction expresses a mass transport in units of kilograms per second. We have for simplicity written this with Cartesian coordinates, but the present analysis is of course made with spherical coordinates. In the atmosphere it is common to use the pressure as a vertical coordinate of the diagnostics, and Eq. (1) can be rewritten using the hydrostatic approximation $dp = -\rho g dz$ so that

$$\Psi(y, p) = \frac{1}{t_1 - t_0} \int_{t_0}^{t_1} \oint \int_0^p \frac{v(x, y, p', t)}{g} dp' dx dt. \quad (2)$$

The vertical integration has been done from the top of the atmosphere down to the isobar p . Thus, $\Psi(y, p)$ is the time-mean meridional mass transport between the pressure p and the top of the atmosphere, whereas $-\Psi(y, p)$ is the transport between p and the surface. Note that the pressure integral is inside the zonal and time average integrals in order to include the zonal and time fluctuations of the surface pressure.

The meridional mass transport streamfunction, with pressure as a vertical coordinate, is shown in the top panel of Fig. 1, where the units are in sverdrups (Sv), defined here as mass transport of 10^9 kg s^{-1} . (Note that this unit is normally used for oceanic volume transport defined as 10^6 m³ s^{-1} , which is close to 10^9 kg s^{-1} for water.)

The integration over the pressure in Eq. (2) can also be made down to the pressure of an isosurface of a selected scalar variable, for example, an isotherm. The general form of the meridional overturning mass transport streamfunction is then

$$\Psi(y, \chi) = \frac{1}{t_1 - t_0} \int_{t_0}^{t_1} \oint \int_0^{p(x, y, \chi, t)} \frac{v(x, y, p', t)}{g} dp' dx dt, \quad (3)$$

where χ is the chosen variable (e.g., the temperature). The vertical integration is still over the pressure so that the unit of the streamfunction remains in sverdrups. When χ is not monotonic with height, it is often more practical to compute $\Psi(y, \chi)$ as

$$\Psi(y, \chi) = \frac{1}{t_1 - t_0} \int_{t_0}^{t_1} \oint \int_0^{p_s(x, y, t)} \frac{v(x, y, p, t)}{g} \mu[\chi'(x, y, p, t) - \chi] dp dx dt, \quad (4)$$

where p_s is the surface pressure and μ is the unit step function. In this general case, $\Psi(y, \chi)$ represents the meridional mass transport in the zonal–height cross section where $\chi(x, y, p, t)$ is greater than the specified value χ .

Two features follows directly from the definition of Eq. (4). To begin with,

$$-\frac{\partial \Psi(y, \chi)}{\partial \chi} d\chi \quad (5)$$

is the time-mean meridional mass transport between the isosurfaces χ and $\chi + d\chi$ in the zonal–vertical plane. Depending on the spatial distribution of χ , the mass transport given by Eq. (5) may occur in a single layer or several disconnected layers, located at different altitudes or longitudes. Second,

$$\frac{\partial \Psi(y, \chi)}{\partial y} dy \quad (6)$$

is the mass transport across the isosurface χ (counted as positive when directed toward increasing χ) in the latitude band between y and $y + dy$. Thus, meridional variations of $\Psi(y, \chi)$ entail mass transport across surfaces of constant χ .

A useful feature is that the meridional transport of the scalar χ can be obtained by integrating $\Psi(y, \chi)$. This can be demonstrated by noting that

$$-\chi \frac{\partial \Psi(y, \chi)}{\partial \chi} d\chi \quad (7)$$

is the transport of χ in the interval χ to $\chi + d\chi$. The total transport is obtained by integrating Eq. (7) over all χ values. Integrating by parts and using the fact that $\Psi(y, \chi)$ vanishes at the integration end points, the meridional transport of χ is obtained as

$$H_\chi(y) = \int_{\chi_{\min}}^{\chi_{\max}} \Psi(y, \chi) d\chi. \quad (8)$$

Here $H_\chi(y)$ is the transport ($\chi \times \text{kg s}^{-1}$) and χ_{\min} and χ_{\max} are the integration limits. Thus, a mass transport streamfunction based on, for example, specific humidity fully specifies the meridional transport of water vapor. This feature of $\Psi(y, \chi)$ will be further considered in connection with meridional energy transport in section 2c.

a. Meridional mass transport streamfunctions

The meridional mass transport streamfunctions, presented in Fig. 1, have been calculated as functions of pressure, temperature, specific humidity, and geopotential height. These streamfunctions describe the time-averaged overturning circulation for the period from 1989 to 2009 and hence give an annual mean picture. The large-scale atmospheric circulation is nearly in hydrostatic balance, and hence the streamfunction with the geopotential height as vertical coordinate is nearly equivalent to the one with pressure as vertical coordinate. In low to middle latitudes, the temperature and the humidity tend to decrease monotonically with altitude locally as well as in the zonal mean (Peixoto and Oort 1992). However, owing to zonal and temporal variations there is no direct relation between the height and the temperature and the humidity. By using these coordinates one captures the mass transport between the ground (or the top of the atmosphere) and a given temperature or humidity surface. [Note that for illustrative purposes, we have in Fig. 1 adopted the convention that positive streamfunction values correspond to anticlockwise circulation. The p , T , and q streamfunctions in this figure have “reversed” vertical axes, implying that Eqs. (5)–(8) must be multiplied by -1 for consistency.]

Figure 1 shows that the mass transport streamfunction in temperature–latitude coordinates comprises two cells in each hemisphere. The tropical (extratropical) cell transports sensible heat equatorward (poleward); see Eq. (8) and the related discussion. The temperature–latitude streamfunction can cross the isothermal surfaces as a result of diabatic heating or due to adiabatic altitude changes. The strength of the tropical Hadley cell circulation in T coordinates is nearly equal to the one obtained in p coordinates. However, the extratropical overturning in T coordinates is significantly stronger than the Ferrel cell overturning in p coordinates. In the extratropical cell, relatively warm lower tropospheric air flows poleward and cools gradually. The temperature decrease of the poleward mass transport with latitude roughly mirrors the zonal-mean meridional temperature gradient near the surface. A difference between the two hemispheres is that, in the northern midlatitudes, the bulk of the poleward transports occurs at temperatures that exceed the annual-mean zonally averaged surface temperature, whereas in the Southern Hemisphere the poleward mass transport is distributed around the mean surface temperature. This mainly reflects the different ratios between land and ocean area in the two hemispheres: in the Northern Hemisphere, where the land fraction is larger, the seasonal cycle is stronger and the zonal variations in surface temperature are more pronounced.

The poleward-flowing branch, at 45°N , has temperatures that spans from about -15° to 15°C . This temperature range is roughly comparable to the winter-mean land–ocean temperature difference; for a lapse rate of $6.5^{\circ}\text{C km}^{-1}$, the temperature range corresponds to an altitude range of about 5 km. However, it should be borne in mind that in connection with surface inversions the temperature increases locally with height. In the extratropical cells, the part of equatorward return flow that is warmer than -30°C first cools, then equatorward of 45°N it begins to warm. To some extent, this equatorward transport is associated with transient near-surface advection of cold air (Held and Schneider 1999). Such transient cold-air outbreaks occur in association with growing baroclinic waves and Rossby wave trains (see, e.g., Lau and Lau 1984).

The T -coordinate mass transport streamfunction reveals that at colder temperatures, typically encountered in the upper troposphere and lower stratosphere, a weaker local cell acts to transport warm (cold) air poleward (equatorward). This cell presumably includes mass transport in the stratosphere where the lapse rate is small. A small temperature difference in this region can be associated with a large altitude difference, which may result in sampling errors. In any event this overturning feature, presumably residing near the tropopause, is not present in the streamfunctions based on pressure and dry or moist static energy (see Fig. 4). One possible reason for this feature is that the thickness-weighted (or eddy induced) velocity is approximately proportional to the inverse vertical gradient of the scalar used to define the layers (Andrews et al. 1987); see also Eq. (15) and the ensuing discussion. Thus, in the stratosphere where the vertical temperature gradient is small, and even can be reversed, it is possible that the transport between isothermal surfaces may be significantly larger than between isentropes.

Figure 1 also shows that the mass transport streamfunction in moisture coordinates comprises two cells in each hemisphere. The boundary between these two cells is located farther equatorward than the cell boundary for the streamfunctions in p and T coordinates. Essentially, this is a consequence of the stronger eddy-induced mass transports in q coordinates (cf. Fig. 3)—an issue that is discussed further in the concluding section. The tropical (extratropical) specific humidity overturning cell fluxes moisture equatorward (poleward). In the tropics, moist air is flowing equatorward in the lower troposphere. Between roughly 15°N and 15°S where the air ascends, the water vapor content decreases owing to condensation. Drier air then flows poleward in the upper troposphere. Essentially, this is a representation in moisture–latitude coordinates of the Hadley cell (Held 2001; Nilsson and Körnich 2008). The ascent and the

TABLE 1. The maximum amplitudes from Fig. 1 of the different cells depending on the chosen vertical coordinate: amplitudes for the Northern and Southern Hemispheres shown as NH/SH. Note that there is only a single Hadley-like cell when the total energy is used as generalized vertical coordinate.

| | Pressure | Temperature | Specific humidity | Geopotential | Total energy |
|--------|----------|-------------|-------------------|--------------|--------------|
| Ferrel | –27/40 | –87/129 | –128/161 | –16/37 | — |
| Hadley | 83/–115 | 87/–114 | 42/–90 | 85/–111 | 140/–163 |

descent, as seen in the decrease and the increase of the humidity, occur essentially at a fixed latitude.

In the extratropics, observations show that the bulk of the poleward moisture transports is carried in narrow, low-level jets associated with cyclones—features referred to as atmospheric rivers (see, e.g., Ralph et al. 2004). The ERA-Interim reanalysis yields an extratropical overturning cell in latitude–humidity coordinates that attains its maximum near 45° latitude. Poleward of this maximum, the entire poleward moving branch becomes drier. Equatorward of the Northern Hemisphere overturning maximum, two type of streamlines can be distinguished. (The situation in the Southern Hemisphere is slightly different.) The part of the poleward transport with a specific humidity exceeding the zonal-mean surface value becomes drier, whereas the part of the transport with a lower specific humidity is moistened. This moistening can occur either when dry parcels descend into the surface boundary layer or as a result of convective mixing in the free troposphere. Near-vertical streamlines presumably characterize the former process, whereas gradually sloping ones characterize the latter process. The nearly linear moisture decrease in the poleward-moving segment at higher latitudes may be partly related to ascent of air in midlatitude cyclones where precipitation occurs (e.g., Ralph et al. 2004). Figure 1 illustrates that the zonal-mean specific humidity gradient at the surface becomes smaller toward the poles. Hence the constant slope of the streamlines may reflect ascending motion, compensating for the decrease in the zonal-mean surface moisture gradient. The equatorward return flow in the extratropics is concentrated at specific humidities below $\sim 2 \text{ g kg}^{-1}$, a value which at 45° latitude is in the zonal mean found near 700 mb. Thus, the overturning in humidity–latitude coordinates primarily reflects the circulation in the lower troposphere.

In summary, the classical picture of the meridional overturning cells appears when the pressure (or the geopotential height) is used as vertical coordinate, with strong Hadley cells, weak Ferrel cells, and even weaker polar cells. Ferrel-like extratropical cells appear also when temperature or specific humidity is used as the vertical coordinate. The intensity of these cells is much stronger than the Ferrel cells in pressure–latitude coordinates. The strongest overturning is obtained in humidity–latitude

coordinates, which has a peak extratropical mass transport of about 140 and 160 Sv in the Northern and Southern Hemispheres, respectively (Table 1). Considering the Hadley cells, comparable overturning strengths are obtained for p and T coordinates, whereas the overturning strength is weaker in specific humidity coordinates.

b. Eddy-induced and mean-flow meridional circulation

When calculating the time-averaged overturning mass transport streamfunction defined by Eq. (3) it is important to take into account that the height for which χ is constant varies in time and space. Therefore, one must integrate the velocity field, first vertically, then zonally, and thereafter over the time to capture the time correlations between the velocity and χ . If, on the other hand, one performs the time averaging separately on the velocity and χ , one obtains a meridional mass transport streamfunction omitting this correlation; hence it represents the contribution of the time-mean circulation. This “mean flow” mass transport streamfunction is defined [see Eq. (4)] as

$$\Psi_M(y, \chi) = \oint \int_0^{p_{SM}(x,y)} \frac{v_M(x, y, p)}{g} \mu [\chi_M(x, y, p) - \chi] dp dx, \quad (9)$$

where p_{SM} , v_M , and χ_M denote time-averaged quantities; for example,

$$v_M(x, y, p) \equiv \frac{1}{t_1 - t_0} \int_{t_2}^{t_1} v(x, y, p, t) dt. \quad (10)$$

Note that the mean-flow overturning is based on the time-mean flow field and the time-mean distribution of the scalar field χ . Note further that no zonal averaging is made, and hence the mean-flow overturning includes contributions from the time-mean zonally averaged circulation as well as from standing eddies (i.e., the correlations between zonal anomalies in the time-mean flow and the time-mean χ field).

Mean-flow mass transport streamfunctions have been calculated for the same period (1989–2009) as the time-averaged streamfunction and are presented in Fig. 2. The results show that the meridional overturning in

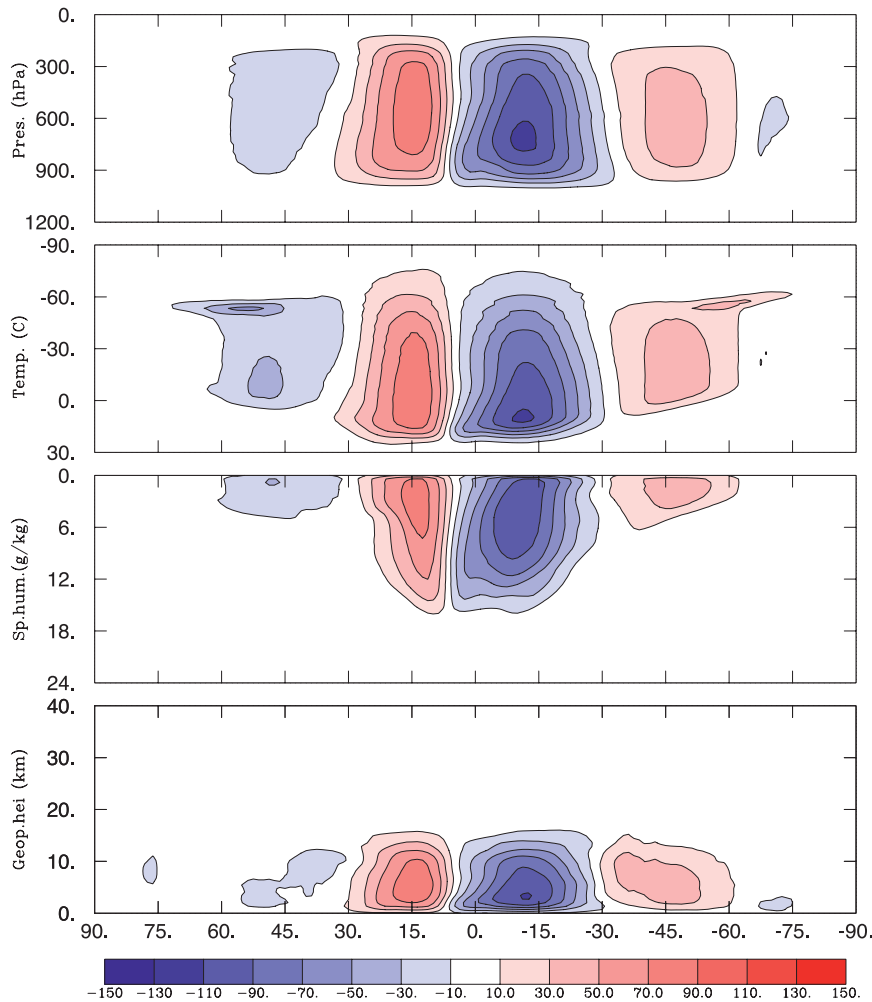


FIG. 2. As in Fig. 1, but for the mean-flow overturning mass transport streamfunctions, which are based on the time-mean velocity and the time-mean generalized vertical coordinate; see Eqs. (9) and (10). Note that, as defined here, the mean-flow components include contributions from standing eddies.

pressure and geopotential coordinates is essentially due to the mean-flow component. In T and q coordinates, the mean-flow and the time-averaged overturning mass transport streamfunctions are of similar strengths within the Hadley cell region, whereas the mean-flow components are weaker in the extratropics where they are comparable to the Ferrel cell strengths of the overturning in pressure coordinates. Note that in the Hadley cell region the overturning due to the mean flow in q coordinates is actually stronger than the time-averaged overturning, which represents the total overturning circulation.

The eddy-induced meridional mass transport streamfunction can now simply be obtained by taking the difference between the time-averaged streamfunction and the mean-flow streamfunction:

$$\Psi_E(y, \chi) = \Psi(y, \chi) - \Psi_M(y, \chi). \quad (11)$$

Figure 3 shows the eddy-induced meridional overturning mass transport streamfunctions. Note that, since the time-averaged streamfunctions represent averages for the period 1989–2009, the eddy-induced streamfunctions include contributions not only from transient eddies but also from the annual cycle and interannual variability. In T and q coordinates, the eddy-induced overturning is composed by a single cell in each hemisphere, which fluxes sensible heat and freshwater, respectively, poleward: warm/moist air flows poleward and colder/drier air returns equatorward. In T coordinates, the eddy-induced overturning is weak in the tropics, where it is concentrated toward high (near surface) temperatures. The weak eddy-induced circulation in the tropics reflects primarily the small horizontal temperature gradients in the free troposphere, which arise because of the weakness of the Coriolis parameter.

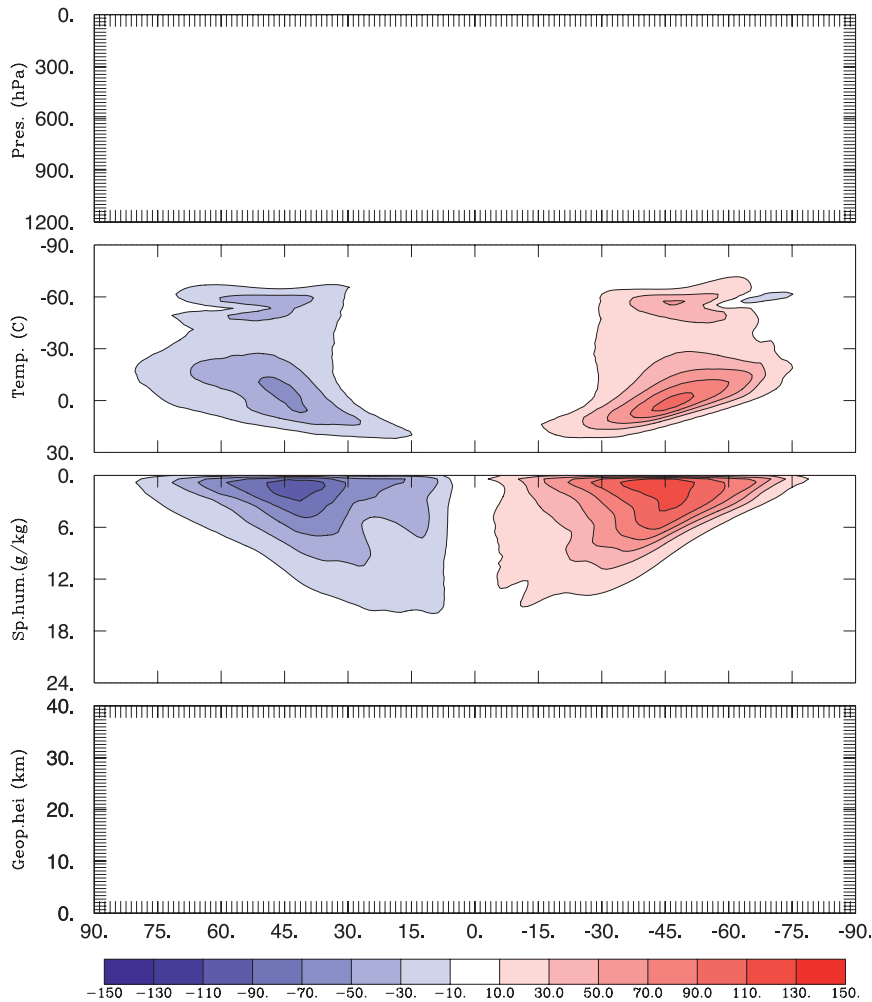


FIG. 3. The eddy-induced meridional mass transport streamfunctions, defined as the difference between Figs. 1 and 2. These streamfunctions result from the time correlation between the meridional velocity and the generalized vertical coordinate and thus include contributions from the seasonal cycle and interannual variability; see Eq. (11). Note that the eddy-induced overturning in pressure and geopotential coordinates are small but nonzero.

The eddy-induced overturning in q coordinates extends essentially to the equator and its mass transport in the midlatitudes is about 50% larger than for the overturning in T coordinates. Also, for the eddy-induced overturning in humidity–latitude coordinates, the poleward-moving branch becomes first gradually moister, then farther poleward gradually drier. In temperature–latitude coordinates, there are weaker secondary overturning maxima at low temperatures, which are encountered around the tropopause.

c. Mass transport streamfunctions as a function of latitude and energy

Linear combinations of the atmospheric variables temperature, geopotential height Z , and specific humidity, variables for which the overturning mass

transport streamfunctions were examined in the previous section, can also be used as the generalized vertical coordinate χ . For hydrostatic flows, the following three energy-related combinations are particularly useful as they tend to be conserved: the dry static energy ($\chi = c_p T + gZ$), which is conserved for dry adiabatic processes; the moist static energy ($\chi = c_p T + gZ + Lq$), which is conserved for moist adiabatic processes; and the latent heat ($\chi = Lq$), which is conserved when the specific humidity is conserved. Figure 4 shows these three energy streamfunctions based on the time average over the period from 1989 to 2005. Here, the temperature is measured in kelvin and the constants used in the computations are the specific heat of dry air $c_p = 1004 \text{ J kg}^{-1} \text{ K}^{-1}$ and the latent heat of evaporation $L = 2501 \text{ J g}^{-1}$ (taken as constant for simplicity). Note that

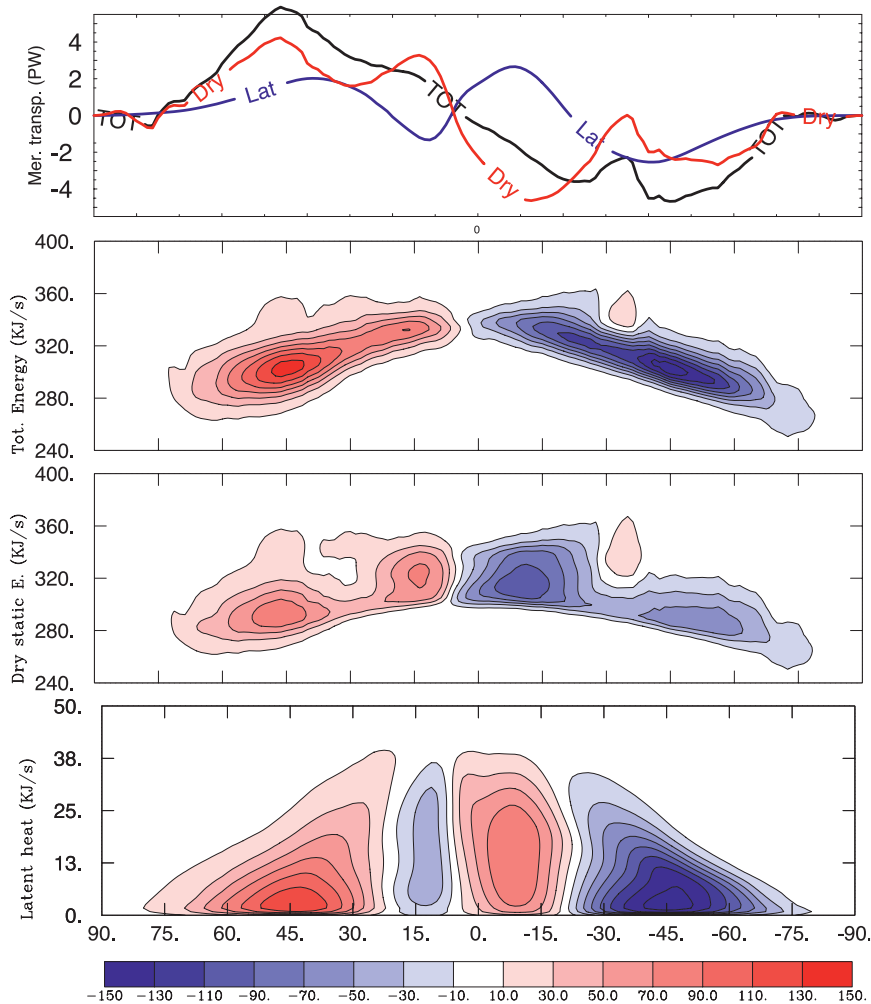


FIG. 4. (top) The meridional energy transport (PW) with dry static energy (red), latent heat (blue), and moist static energy (black). The meridional overturning mass transport streamfunction (Sv) as a function of (top middle) moist static energy, (bottom middle) dry static energy, and (bottom) latent heat: streamlines every 20 Sv; positive streamfunction values correspond to anticlockwise circulation.

the moist static energy mass transport streamfunction is not the sum of the streamfunctions in dry static and latent energy coordinates.

The mass transport streamfunctions based on the potential temperature and the equivalent potential temperature are qualitatively similar to the ones obtained when using the dry or the moist static energy, respectively (e.g., Held and Schneider 1999; Czaja and Marshall 2006; Pauluis et al. 2010). One advantage of the mass transport streamfunctions in energy coordinates, however, is their close relation to the meridional energy transport. In the top panel of Fig. 4, the meridional transports of latent heat and dry and moist static energy are illustrated. These transports can be calculated as

$$H_{\chi}(y) = \frac{1}{t_1 - t_0} \int_{t_0}^{t_1} \oint \int_0^{p_s} \chi(x, y, p, t) v(x, y, p, t) \frac{dp}{g} dx dt, \quad (12)$$

where χ represents one of the energy variables (i.e., the moist static, the dry static, or the latent energy). Alternatively, the meridional energy transports can be obtained directly from the corresponding overturning mass transport streamfunctions; Eq. (8) shows that the area under the streamfunction in the χ direction equals the meridional transport of the quantity χ . It is straightforward to show that if the mean-flow streamfunction $\Psi_M(y, \chi)$ is used in Eq. (8), then the mean-flow contribution to the energy transport is obtained:

$$\int_{\chi_{\min}}^{\chi_{\max}} \Psi_M(y, \chi) d\chi = \oint \int_0^{p_s} \chi_M(x, y, p) v_M(x, y, p) \frac{dp}{g} dx. \quad (13)$$

A similar relation applies for the eddy-induced energy transport.

The present ERA-Interim-based mass transport streamfunctions with moist static and dry static energy coordinates, shown in Fig. 4, are similar to the National Centers for Environmental Prediction (NCEP)-based streamfunctions presented by Czaja and Marshall (2006). For these two latitude–energy streamfunctions, the overturning consists of one cell in each hemisphere. Further, the overturning is thermally direct in the sense that the energy content of the poleward-flowing air is greater than that of the equatorward-flowing air. Generally, the poleward isoline slope of the moist static energy overturning is more pronounced than that of the dry static energy overturning. The reason is that for poleward-moving air in the free troposphere, the decline in dry static energy due to radiative cooling is partly countered by latent heating, whereas the decline in moist static energy reflects only the radiative cooling. In the tropics, where the vertical difference in moist static energy generally is small, the overturning in moist static energy spans a smaller energy difference than the overturning in dry static energy (Held 2001; Czaja and Marshall 2006). The strong flow toward higher dry static energy near the equator, associated with the ascending branch of the Hadley circulation, is mainly due to latent heating. This feature is less pronounced when the overturning is viewed in moist static energy coordinates, as the near-equatorial ascent is nearly moist adiabatic. It should be recalled that the moist static energy in the tropics has a midtropospheric minimum at ~ 600 hPa (Xu and Emanuel 1989; Czaja and Marshall 2006). Thus, there is not necessarily a direct relationship between the overturning in moist static energy coordinates and the overturning in geometrical coordinates. However, for deep thermally direct tropical circulations, the upper tropospheric branch has generally a higher moist static energy content than the near-surface branch (e.g., Emanuel et al. 1994; Nilsson and Emanuel 1999; Held 2001).

Figure 4 shows that in the extratropics, the moist static energy overturning is stronger than the dry static overturning. Analyses presented by Pauluis et al. (2008, 2010) show that the moist static energy representation better separates poleward- and equatorward-moving air parcels in the midlatitudes and hence yields a stronger mass transport. For the baroclinic eddies that dominate the midlatitude mass transport, there is thus less cancellation between the warm (high energy) poleward-moving sector and the cold (low energy) equatorward-moving

sector when the net meridional mass transport is calculated in moist static energy (or equivalent potential temperature) layers. It is interesting to note that, in the midlatitudes, the overturning based on specific humidity is roughly as strong as the one based on moist static energy. Hence, also the specific humidity mass transport streamfunction, which should sample the flow in low-level jets (Ralph et al. 2004), separates the poleward- and the equatorward-moving air better than the streamfunctions based on dry static energy or temperature.

The overturning mass transport streamfunctions in energy coordinates have also been decomposed into a mean-flow part, shown in Fig. 5, and an eddy-induced part, shown in Fig. 6. Generally, the mean-flow contributions to the energy streamfunctions are strong in the tropics and weak in the extratropics. The moist static energy representation of the mean-flow overturning yields the weakest Hadley cells. This is presumably related to the lower tropospheric minimum in moist static energy: midtropospheric air that flows poleward between about 400 and 600 hPa tends to have a moist static energy content that is comparable to equatorward-flowing air at slightly lower altitudes. In the midlatitudes of the Southern Hemisphere the mean-flow overturning in moist- and dry-static energy coordinates are thermally indirect, implying that they carry energy equatorward. In the midlatitudes of the Northern Hemisphere, on the other hand, these overturning mass transport streamfunctions are thermally direct but weak. The reason is the stronger energy transport due to stationary waves in the Northern Hemisphere (see, e.g., Peixoto and Oort 1992), which yields a thermally direct mean-flow overturning in moist- and dry-static energy coordinates. The eddy-induced overturning mass transport streamfunctions peak around 45° latitude. The strongest overturning is obtained when the moist static energy is used as a vertical coordinate; the latent energy yields an overturning of intermediate strength and the dry static energy yields the weakest overturning.

3. Discussion

Based on the ERA-Interim reanalysis data, the atmospheric circulation has been examined by computing meridional overturning mass transport streamfunctions with generalized vertical coordinates. The novel contributions of the present paper include analyses of the overturning in temperature and humidity coordinates and the separation of the generalized overturning mass transport streamfunctions in mean-flow and eddy-induced components.

One noteworthy result is that all the computed streamfunctions have a fairly simple structure with one poleward

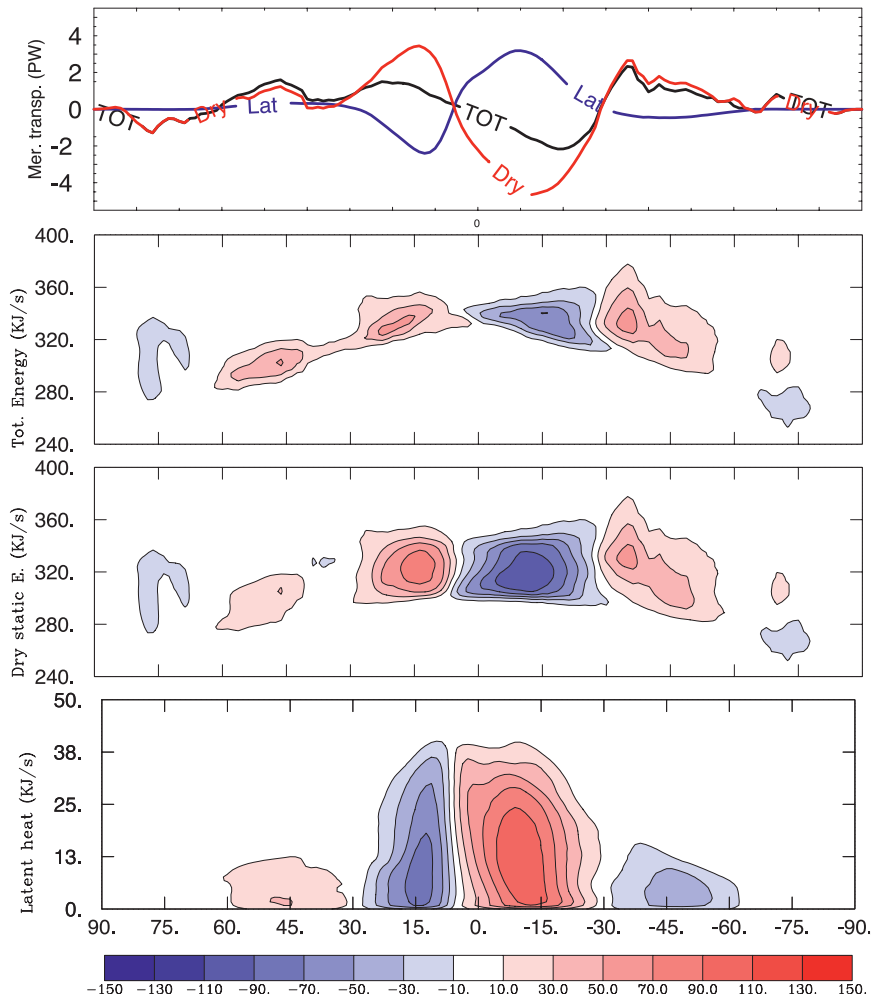


FIG. 5. As in Fig. 4, but for the mean-flow contributions; see Eqs. (9) and (10).

branch and one equatorward branch (the exception is the secondary maxima around the tropopause seen in the T -coordinate overturning). Thus, the meridional overturning circulation has essentially a “two-layer” structure regardless of whether the pressure, the temperature, the specific humidity, the dry static energy, or the moist static energy is used as independent variable. This is true for the total streamfunctions as well as their mean-flow and eddy-induced components.

The latitudinal structure of the mass transport streamfunctions, on the other hand, depends on the choice of the generalized vertical coordinate. The total streamfunctions based on pressure, temperature, and specific humidity have distinct tropical and extratropical overturning cells, whereas the ones based on dry and moist static energy tend to have a single hemispheric overturning cell. One might suspect that this difference reflects that the dry and moist static energies are more conserved and that the corresponding streamfunctions therefore better capture

the Lagrangian circulation. Following trajectories, however, the specific humidity should in general be nearly as conserved as the dry static energy. The physics controlling whether a one- or a two-cell structure emerges can be illuminated by considering the residual circulation related to a tracer $\chi(x, y, z, t)$ (see Andrews et al. 1987, chapter 9.4). Note that this residual circulation is an approximation in geometrical coordinates of the mass transport streamfunction based on the tracer χ (McDougall and McIntosh 1996; McIntosh and McDougall 1996). For the purpose of illustration, we consider an incompressible Boussinesq flow in z coordinates. The streamfunction for the residual velocity field is

$$\psi_*(y, z) = \psi(y, z) + \psi_e(y, z). \quad (14)$$

Here $\psi(y, z)$ is the zonally averaged Eulerian streamfunction, representing the conventional Hadley–Ferrel

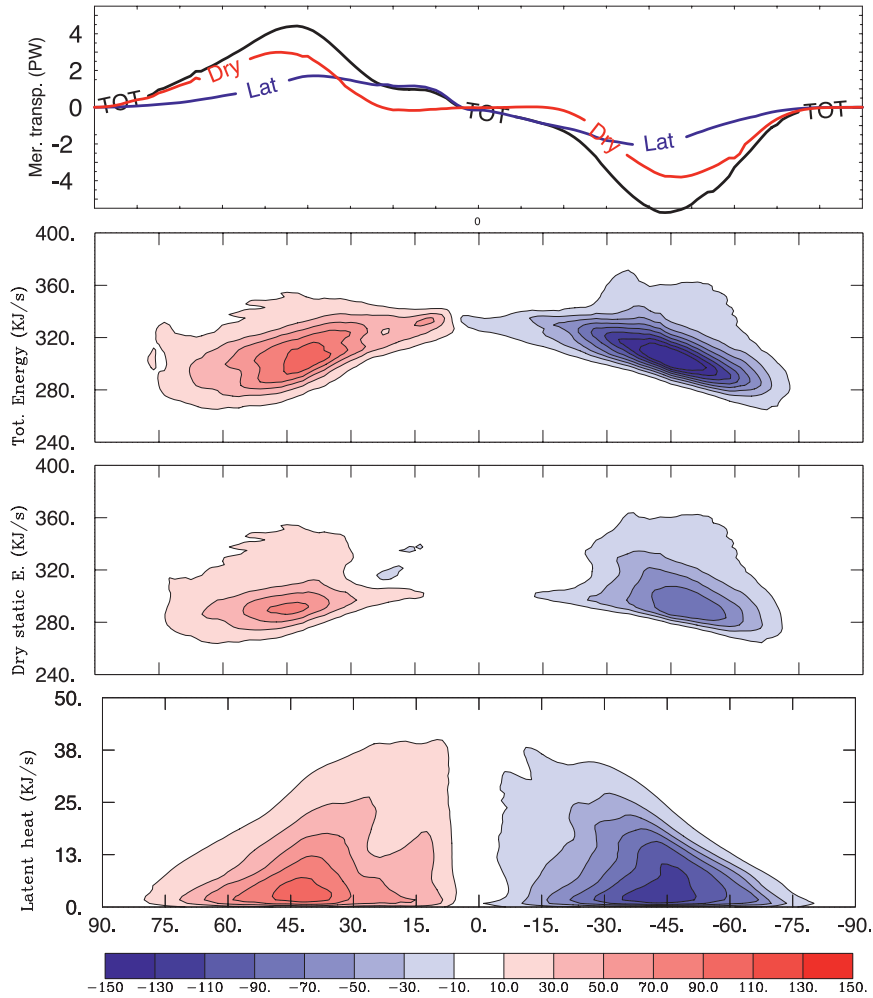


FIG. 6. As in Fig. 4, but for the eddy-induced contributions, which include all time-dependent flow components. Note the weak equatorward transport of dry static energy in the tropics, which is due to the seasonal migration of the ascending branch of the Hadley cell.

cell circulation, and $\psi_e(y, z)$ is the eddy-induced streamfunction. The residual velocity field is given by $(v_*, w_*) = (-\partial_z \psi_*, \partial_y \psi_*)$, and similarly for the Eulerian and eddy-induced fields. In the limit of small zonal fluctuations of χ , one obtains the standard form (Andrews and McIntyre 1976; Plumb and Ferrari 2005)

$$\psi_e(y, z) = \frac{\overline{v'\chi'}}{\overline{\chi'_z}}, \quad (15)$$

where the overbar and the prime denote the zonal mean and fluctuations, respectively, and $\overline{\chi'_z}$ the vertical gradient.

We now consider the zonal-mean overturning in the Northern Hemisphere and examine qualitatively the residual circulations that result when χ is taken to be the dry static energy (or the potential temperature) and

the specific humidity, respectively. For the dry static energy s , observations² show that $\overline{v's'} > 0$ and $\overline{s'_z} > 0$, implying that $\psi_e > 0$. As a result, the eddy-induced overturning ψ_e acts to reinforce the Hadley cell for which $\psi > 0$, but to curtail the Ferrel cell for which $\psi < 0$. The resulting residual circulation is characterized by a single thermally direct cell [cf. Held and Schneider (1999) for an illustration of ψ_* based on potential temperature]. In the case of specific humidity, observations show that $\overline{v'q'} > 0$ and $\overline{q'_z} < 0$ (see Peixoto and Oort 1992, Figs. 12.4 and 12.11), implying that $\psi_e < 0$. In this case, the eddy-induced overturning acts to curtail the Hadley cell but to reinforce the Ferrel cell. We are not

² The eddy flux of dry static energy is dominated by the sensible heat component (i.e., $\overline{v's'} \approx c_p \overline{v'T'}$) (see Peixoto and Oort 1992, Figs. 13.6 and 13.7).

aware of any published computations of the residual circulation related to specific humidity. However, it is evident that this residual circulation will have a Ferrel-like midlatitude cell with poleward flow near the surface and equatorward flow aloft: this structure is required to obtain a poleward transport of specific humidity. The residual streamfunction related to temperature is expected to have a similar pattern since in the most of the troposphere $\bar{T}_z < 0$. This reasoning shows that for the residual circulation related to q or T there is a tropical Hadley-like cell and an extratropical Ferrel-like cell. Furthermore, the eddy-induced overturning acts to move the Hadley–Ferrel cell boundary of the residual circulation equatorward relative to the cell boundary of the zonal-mean Eulerian overturning.

Reasoning similar to that given above can be invoked to explain the meridional-cell structure of the overturning mass transport streamfunctions. The eddy-induced components are basically downgradient in the sense that they transport temperature (i.e., sensible heat) and specific humidity as well as dry and moist static energy poleward; see Fig. 6 and Eq. (8). For the mean-flow component, on the other hand, the meridional direction of the resulting energy transports can differ: in the Hadley cell region, for example, the mean-flow component transports dry static energy (which increases with height) poleward but specific humidity (which decreases with height) equatorward; cf. Fig. 5. Thus, also for the overturning mass transport streamfunctions, the meridional-cell structure depends on whether the mean-flow and the eddy-induced components reinforce or curtail each other. The fact that the Hadley cell is narrower in the q representation than in the T representation in Fig. 1 simply reflects that the eddy-induced mass transport streamfunction is stronger in the former.

For the mass transport streamfunction based on dry static energy, the equatorward mass transport in mid-latitudes occurs at low energies, which are associated with temperatures that are lower than the time-mean zonally averaged surface temperature (Held and Schneider 1999; Czaja and Marshall 2006). Held and Schneider pointed out that this equatorward near-surface mass transport is accomplished primarily by transient cold air outbreaks, occurring in association with baroclinic instability or Rossby wave trains (e.g., Lau and Lau 1984). At around 45°N, the eddy-induced T -coordinate streamfunction yields an equatorward mass transport of air that is colder than about -5°C . This equatorward transport includes contributions from transient near-surface advection of cold air, but poleward mass transport above the surface in the same temperature interval makes the equatorward eddy-induced mass transport in temperature coordinates smaller than in dry static energy coordinates;

see Figs. 3 and 6. Conceptual figures of the zonal–vertical structure in transient eddies that illustrate the mass transport in isentropic layer can be found in, for example, Townsend and Johnson (1985) and Grotjahn (1993).

Pauluis et al. (2008, 2010) have proposed a slightly revised version of the global atmospheric circulation to explain why the overturning based on moist static energy is stronger than the one based on dry static energy. They emphasize a circulation component that originates near the surface in the subtropics and involves warm moist parcels that are carried poleward by eddies into the midlatitude storm tracks. Here, these air parcels ascend into the upper troposphere and continue poleward. Essentially, the reason for the difference in overturning strengths in midlatitudes is that air in the lower troposphere with nearly the same dry static energy is flowing poleward as well as equatorward (Pauluis et al. 2010). However, the poleward-moving air generally has a higher specific humidity than the equatorward-moving air. This causes the meridional mass transport to be larger when computed within specific humidity or moist static energy layers than when computed within dry static energy layers. Some features of the “moist” branch described by Pauluis et al. (2008) can be seen in the meridional overturning in specific humidity coordinates: Fig. 6 is suggestive of the eddy-induced circulation component that collect moisture under “descent” in the subtropics and deposit moisture under “ascent” in the extratropics.

One benefit of computing an overturning mass transport streamfunction for a scalar field χ is that it describes the strength of the flow component that carries the tracer meridionally as well as the tracer difference over which the flow operates. The meridional transport of χ can be written in the form

$$H_\chi(y) = \Delta\chi(y)\Psi_\chi(y), \quad (16)$$

where Ψ_χ characterizes the strength of $\Psi(y, \chi)$ and $\Delta\chi$ is a flow-weighted difference. One way to define these quantities is to let Ψ_χ be the maximum (or when appropriate the minimum) of $\Psi(y, \chi)$ and use Eq. (16) to obtain $\Delta\chi \equiv H_\chi/\Psi_\chi$. As an illustration, we have calculated these transport-related quantities from the streamfunction with specific humidity as independent variable: Fig. 7 shows that the interhemispheric differences in meridional water vapor transport primarily are controlled by the strength of the mass transport, although there are interhemispheric differences in Δq . Analyses of this kind, based on the streamfunction $\Psi(y, q)$, should be highly suitable for examining variability and changes of the hydrological cycle in data and models [see, e.g., the study of Held and Soden (2006)]. The fact that a change in the water vapor transport can be

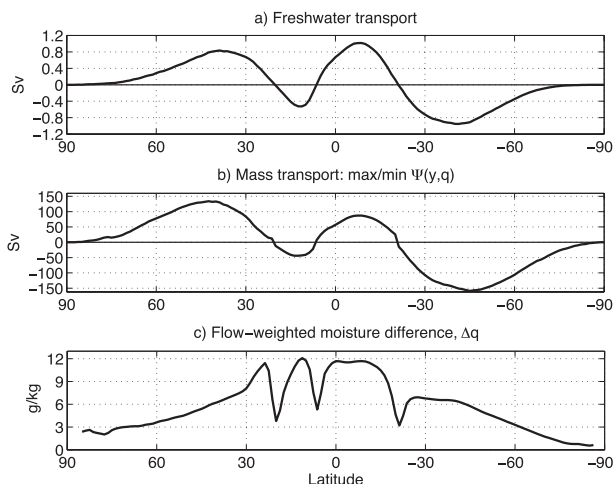


FIG. 7. An analysis of the meridional water vapor (freshwater) transport based on the specific humidity streamfunction $\Psi(y, q)$: (a) water vapor transport $H_q(y)$, proportional to the latent heat transport shown in Fig. 4; (b) Maximum northward/southward mass transport of $\Psi(y, q)$ as a function of latitude; and (c) flow-weighted moisture difference computed as $\Delta q = H_q(y)/[\max/\min \Psi(y, q)]$ (see the text for details). The sign convention follows Eqs. (5)–(8); positive mass transport values correspond to northward water vapor transport.

separated into components due to flow and moisture-range changes can yield information on the underlying changes of the general circulation. Potentially, streamfunction-based analyses of passive tracers with latitudinally distributed sources and sinks could be of interest and possibly yield additional information on the atmospheric circulation.

As a closing remark, overturning mass transport streamfunctions based on temperature and specific humidity for the individual seasons should yield a somewhat sharper image of the general circulation than the annual-mean streamfunctions, which have been the scope of the present study. Thus, one natural extension of the present work is to examine seasonally averaged streamfunctions and to further decompose the mean-flow contribution into zonal-mean and standing-eddy components.

Acknowledgments. The work reported here was supported by the Swedish Research Council and is a contribution from the Bert Bolin Centre for Climate Research at Stockholm University. We thank Rodrigo Caballero and Peter Langen for discussions and two anonymous reviewers for constructive comments.

REFERENCES

Andrews, D. G., and M. E. McIntyre, 1976: Planetary waves in horizontal and vertical shear: The generalized Eliassen–Palm

- relation and the mean zonal acceleration. *J. Atmos. Sci.*, **33**, 2031–2048.
- , J. R. Holton, and C. B. Leovy, 1987: *Middle Atmosphere Dynamics*. Academic Press, 489 pp.
- Bryan, K., and J. L. Sarmiento, 1985: Modeling ocean circulation. *Advances in Geophysics*, Vol. 28, Academic Press, 433–459.
- Czaja, A., and J. Marshall, 2006: The partitioning of poleward heat transport between the atmosphere and ocean. *J. Atmos. Sci.*, **63**, 1498–1511.
- Diaz, H. F., and R. S. Bradley, 2004: *The Hadley Circulation: Present, Past and Future*. Springer, 511 pp.
- Döös, K., and D. J. Webb, 1994: The Deacon cell and the other meridional cells in the Southern Ocean. *J. Phys. Oceanogr.*, **24**, 429–442.
- , J. Nycander, and A. C. Coward, 2008: Lagrangian decomposition of the Deacon cell. *J. Geophys. Res.*, **113**, C07028, doi:10.1029/2007JC004351.
- Emanuel, K. A., J. D. Neelin, and C. S. Bretherton, 1994: On large-scale circulations in convecting atmospheres. *Quart. J. Roy. Meteor. Soc.*, **120**, 1111–1143.
- Grotjahn, R., 1993: *Global Atmospheric Circulations: Observation and Theories*. 1st ed. Oxford University Press, 430 pp.
- Held, I. M., 2001: The partitioning of the poleward energy transport between the tropical ocean and atmosphere. *J. Atmos. Sci.*, **58**, 943–948.
- , and T. Schneider, 1999: The surface branch of the zonally averaged mass transport circulation in the troposphere. *J. Atmos. Sci.*, **56**, 1688–1697.
- , and B. J. Soden, 2006: Robust responses of the hydrological cycle to global warming. *J. Climate*, **19**, 5686–5699.
- Hirst, A. C., D. R. Jackett, and T. J. McDougall, 1996: The meridional overturning cells of a World Ocean model in neutral coordinates. *J. Phys. Oceanogr.*, **26**, 775–791.
- Karoly, D. J., P. C. McIntosh, P. Berrisford, T. J. McDougall, and A. C. Hirst, 1997: Similarities of the Deacon cell in the Southern Ocean and Ferrel cells in the atmosphere. *Quart. J. Roy. Meteor. Soc.*, **123**, 519–526.
- Lau, N.-C., and K.-M. Lau, 1984: The structure and energetics of midlatitude disturbances accompanying cold-air outbreaks over East Asia. *Mon. Wea. Rev.*, **112**, 1309–1327.
- Lichtenberg, A. J., and M. A. Lieberman, 1983: *Regular and Stochastic Motion*. Springer-Verlag, 499 pp.
- Marshall, J., and T. Radko, 2006: A model of the upper branch of the meridional overturning of the Southern Ocean. *Prog. Oceanogr.*, **70**, 331–345.
- McDougall, T. J., and P. C. McIntosh, 1996: The temporal-residual-mean velocity. Part I: Derivation and the scalar conservation equations. *J. Phys. Oceanogr.*, **26**, 2653–2665.
- McIntosh, P. C., and T. J. McDougall, 1996: Isopycnal averaging and the residual mean circulation. *J. Phys. Oceanogr.*, **26**, 1655–1660.
- Nilsson, J., and K. A. Emanuel, 1999: Equilibrium atmospheres of a two-column radiative–convective model. *Quart. J. Roy. Meteor. Soc.*, **125**, 2239–2264.
- , and H. Körnich, 2008: A conceptual model of the surface salinity distribution in the oceanic Hadley cell. *J. Climate*, **21**, 6586–6598.
- Pauluis, O., A. Czaja, and R. Korty, 2008: The global atmospheric circulation on moist isentropes. *Science*, **321**, 1075–1078.
- , —, and —, 2010: The global atmospheric circulation in moist isentropic coordinates. *J. Climate*, **23**, 3077–3093.
- Peixoto, J. P., and A. H. Oort, 1992: *Physics of Climate*. Springer-Verlag, 520 pp.

- Plumb, R. A., and R. Ferrari, 2005: Transformed Eulerian-mean theory. Part I: Nonquasigeostrophic theory for eddies on a zonal-mean flow. *J. Phys. Oceanogr.*, **35**, 165–174.
- Ralph, F. M., P. J. Neiman, and G. A. Wick, 2004: Satellite and Caljet aircraft observations of atmospheric rivers over the eastern North Pacific Ocean during the winter 1997/98. *Mon. Wea. Rev.*, **132**, 1721–1745.
- Simmons, A., S. Uppala, D. Dee, and S. Kobayashi, 2007a: ERA-Interim: New ECMWF reanalysis products from 1989 onwards. *ECMWF Newsletter*, No. 110, ECMWF, Reading, United Kingdom, 25–35.
- , —, and —, 2007b: Update on ERA-Interim. *ECMWF Newsletter*, No. 111, ECMWF, Reading, United Kingdom, 5.
- Townsend, R. D., and D. R. Johnson, 1985: A diagnostic study of the isentropic zonally averaged mass circulation in the first GARP global experiment. *J. Atmos. Sci.*, **42**, 1565–1579.
- Uppala, S. M., and Coauthors, 2005: The ERA-40 Re-Analysis. *Quart. J. Roy. Meteor. Soc.*, **131**, 2961–3012.
- , D. Dee, S. Kobayashi, P. Berrisford, and A. Simmons, 2008: Towards a climate data assimilation system: Status update of ERA-Interim. *ECMWF Newsletter*, No. 115, ECMWF, Reading, United Kingdom, 12–18.
- Xu, K.-M., and K. A. Emanuel, 1989: Is the tropical atmosphere conditionally unstable? *Mon. Wea. Rev.*, **117**, 1471–1479.